

Ion dynamics in helicon sources^{a)}

J. L. Kline,^{b)} M. M. Balkey, and P. A. Keiter
Los Alamos National Laboratory, Los Alamos, New Mexico 87545

E. E. Scime, A. M. Keesee, X. Sun, R. Hardin, and C. Compton
Physics Department, West Virginia University, Morgantown, West Virginia 26505

R. F. Boivin
Physics Department, Auburn University, Auburn, Alabama 36849

M. W. Zintl
Scientific Applications & Research Associates Inc., Huntington Beach, California 92649

(Received 7 November 2002; accepted 30 January 2003)

Recent experiments have demonstrated that phenomena associated with ion dynamics, such as the lower hybrid resonance, play an important role in helicon source operation. In this work, a review of recent ion heating measurements and the role of the slow wave in heating ions at the edge of helicon sources is presented. The relationship between parametrically driven waves and ion heating near the rf antenna in helicon sources is also discussed. Recent measurements of parallel and rotational ion flows in helicon sources are presented and the implications for particle confinement, instability growth, and helicon source operation are reviewed. © 2003 American Institute of Physics. [DOI: 10.1063/1.1563260]

I. INTRODUCTION

The first helicon source was built as a basic plasma research tool to investigate the left-handed circularly polarized, whistler, wave in magnetized plasmas.¹ Although the left-handed, circularly polarized wave was not observed, those initial experiments demonstrated that the helicon source generated relatively high densities for laboratory plasmas, $n \sim 10^{12} \text{ cm}^{-3}$, with a large ionization fraction. Except for a few magnetoplasma experiments,^{2,3} little interest was shown in the helicon source until the mid-1980's, when silicon chip manufacturing began to grow rapidly. The relatively high densities and large ionization fraction for moderate input powers made the helicon source a good candidate for an advanced plasma-processing source. The primary goal of experiments on helicon sources until the late 1990's was optimization for plasma processing.

Since the late 1990's, helicon sources have been used as plasma sources for research in many areas of plasma physics including: space-relevant, high-beta studies;⁴ plasma propulsion;⁵ and basic plasma science.^{6,7} One problem associated with employing helicon sources in many of these research areas is that the essential physics of helicon sources has been poorly understood until only recently. Initial theoretical investigations of helicon sources focused on the excitation of bounded whistler, helicon, waves and the dynamics of electrons in those waves.^{8,9} Later theoretical studies included the effects of the slower root to the cold plasma dispersion relation in a bounded cylinder, the so-called Trivelpiece–Gould mode.^{10–12} Helicon waves are the faster

phase velocity solution to the cold plasma dispersion relation.

Although the early experiments were performed at rf near the lower hybrid frequency (a frequency that is routinely used to heat ions in thermonuclear fusion experiments) and later experiments indicated that ion dynamics near the lower hybrid frequency could play an important role in helicon sources,¹³ ion dynamics in helicon sources has been largely ignored in theoretical studies. Some early theoretical studies did note that, near the lower hybrid frequency, ion motion effects could substantially alter the cold plasma dispersion relation.¹⁴ However, since only the slow wave has a resonance at the lower hybrid frequency, the theoretical studies of helicon wave propagation typically ignored ion effects by only examining solutions for frequencies much higher than the lower hybrid frequency and assuming that the ions are cold (less than 0.1 eV),¹⁵ that they flow out the end of linear helicon sources at the sound speed, and that they have no significant rotational flow.¹⁶ The lower hybrid frequency, ω_{lh} , is defined as

$$1/\omega_{\text{lh}}^2 = 1/(\omega_{ce}\omega_{ci}) + 1/(\omega_{pi}^2 + \omega_{ci}^2), \quad (1)$$

where ω_{pi} is the ion plasma frequency, ω_{ci} is the ion cyclotron frequency, and ω_{ce} is the electron cyclotron frequency. In this paper, we summarize a series of experiments that have examined ion heating and ion flows in the West Virginia University helicon source. The experimental apparatus is described in Sec. II. Ion heating observations and their relationship to slow wave resonances and parametrically driven waves are reviewed in Sec. III. Recent ion flow measurements are described in Sec. IV and the significance of ion effects in terms of helicon source operation is discussed in Sec. V.

^{a)}Paper CI 2 1, Bull. Am. Phys. Soc. **47**, 56 (2002).

^{b)}Invited speaker. Electronic mail: jkline@lanl.gov

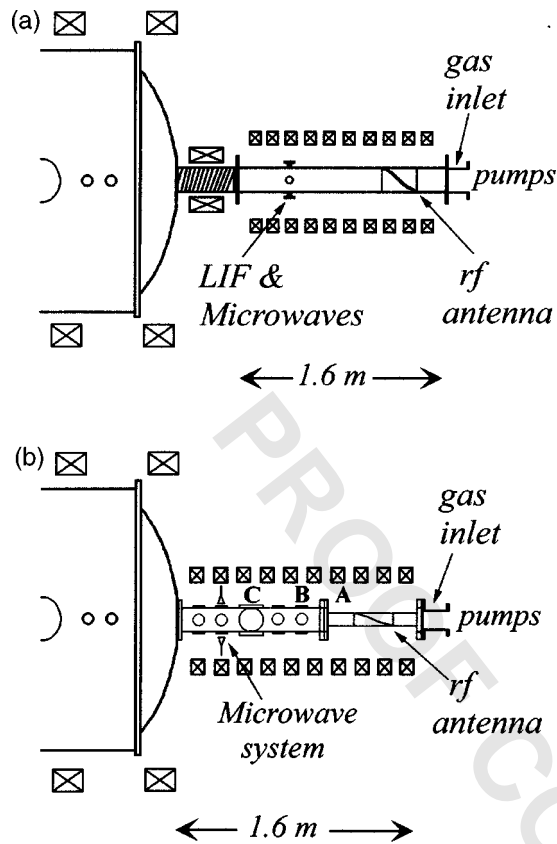


FIG. 1. Schematic diagrams of (a) HELIXa and (b) HELIXb.

II. EXPERIMENTAL APPARATUS

Ion dynamics experiments have been performed using two different helicon source plasma chambers on the hot helicon experiment (HELIX) at West Virginia University. The first chamber, HELIXa [Fig. 1(a)], was a Pyrex™ tube that was 157 cm long and 15 cm in diameter.¹³ The all glass tube had a single set of four $2\frac{3}{4}$ in. crossing ports 57 cm from the front edge of the antenna. The second chamber, HELIXb [Fig. 1(b)], was a hybrid chamber consisting of a 60-cm-long, 10-cm-diam Pyrex™ section connected to a 100-cm-long, 15-cm-diam stainless steel section.¹⁷ The stainless steel section had one set of four 6 in. crossing ports and four sets of four $2\frac{3}{4}$ in. crossing ports. The other end of the stainless steel chamber was connected to a large, 2-m-diam, 4-m-long space simulation chamber (LEIA).⁴ The other end of the glass section of the chamber was connected to a 540 l/s turbomolecular drag pumping station. Fill gas was added through an inlet between the glass section and the pumping station. A 19 cm, $m = +1$ helical antenna driven with an ENI 30 dB, 2 kW rf amplifier was used to generate the argon plasma.

The HELIX chambers were typically surrounded by ten electromagnets capable of providing a uniform axial magnetic field of up to 1185 G. For all the experiments described here, the LEIA magnetic field was fixed at 36 G. HELIXb was operated in two different magnetic field configurations, a ten-magnet coil configuration and an eight-magnet coil configuration. In the eight-coil configuration, the last two elec-

tromagnets between HELIXb and LEIA were disconnected. Removing the two coils allowed the eight-coil configuration to reach magnetic fields of 1300 G.¹⁷ However, in the eight-coil configuration, the outer magnetic field lines ($r > 3.5$ cm) intersect the wall of the stainless steel chamber near the junction with the LEIA chamber, thereby imposing a partially conducting axial boundary. Because HELIXa was connected to LEIA via a 6 in. stainless steel bellows, while the stainless steel chamber of HELIXb was directly connected to LEIA, the additional distance between HELIXa and LEIA also resulted in outer magnetic field lines intersecting conducting bellows walls. Therefore, the axial boundary conditions in the HELIXa and eight-coil HELIXb experiments were somewhat similar. With HELIXb in the ten-coil configuration, nearly all the magnetic field lines terminated on the inner conducting walls of LEIA. Although no specific work has been done to study the effect of axial boundary conditions on ion heating, HELIXb ion temperatures were significantly higher in the eight-coil configuration than in the ten-coil configuration for the same magnetic field strength, 0.75 eV vs 0.35 eV. Thus, the magnetic field geometry within a given helicon source vacuum chamber can play an important role in ion heating.

Electron temperatures and densities were measured with a rf compensated Langmuir probe.¹⁸ Density measurements were confirmed on a subset of plasma parameters with steady state microwave interferometry.¹⁹ Ion temperatures and flows, both parallel and perpendicular to the applied magnetic field, were obtained from direct measurements of the ion velocity distribution function by laser induced fluorescence (LIF).^{20,21} In HELIXa, the LIF measurements could only be performed at a single axial point 57 cm from the front edge of the antenna in both perpendicular and parallel directions.²² In HELIXb, the LIF measurements were typically performed at the axial positions labeled A, B, and C in Fig. 1(b), where position A was 5 cm, position B was 35 cm, and position C was 66 cm from the front of the antenna. At position C, LIF measurements could be made over a two-dimensional cross of the plasma column. Details of the LIF system for HELIXa and HELIXb have been published elsewhere.^{13,17} The electrostatic fluctuation measurements were made with a fixed pair of probes at axial position “B.” The electrostatic probe consisted of two Langmuir probe tips separated by 5.8 mm. So that high frequency floating potential fluctuations could be measured, the electrostatic probe tips were not rf compensated.

III. ION HEATING IN HELICON PLASMAS

Several key characteristics of ion heating have been observed in helicon plasmas: anisotropic ion temperatures that peak at particular values of applied magnetic field and rf, an axial ion temperature profile peaked downstream from the antenna, and a strong correlation with the lower hybrid frequency. Measurements of these characteristics suggest the one possible mechanism for ion heating in helicon plasmas is the slow wave or “Trivelpiece–Gould” mode. Electrostatic

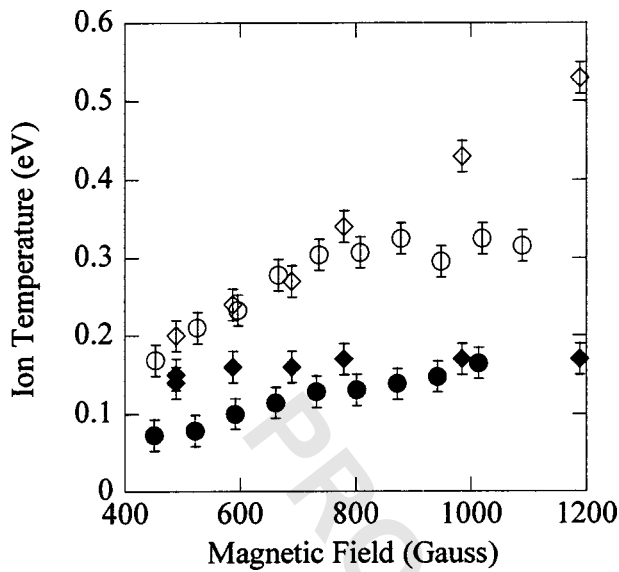


FIG. 2. (\diamond) Perpendicular and (\blacklozenge) parallel ion temperature measurements as a function of magnetic field strength in HELIXa for a fill pressure of 2 mTorr, a rf driving frequency of 9 MHz and a rf power of 400 W. (\circ) Perpendicular and (\bullet) parallel ion temperature measurements as a function of magnetic field strength in HELIXb for a fill pressure of 6.7 mTorr, a rf driving frequency of 9 MHz and a rf power of 750 W.

probe measurements of wave spectra show that another ion heating mechanism may be the parametric decay of the helicon wave.

A. Characteristics of the ion temperatures in HELIX

The anisotropic ion temperatures measured in HELIXa were completely unexpected given the large ion-ion collision frequencies in dense helicon plasmas. That energy is coupled into the ions in a preferential direction provides a critical clue as to the origin of ion heating in helicon sources. Our initial study of the ion temperatures demonstrated that the ion temperature anisotropy scaled linearly with the magnetic field strength.²² The on-axis perpendicular ion temperature increased linearly with magnetic field while the parallel ion temperature remained about the same. Perpendicular and parallel ion temperatures versus magnetic field strength in HELIXa (from Scime *et al.*²²) along with measurements in HELIXb in the ten-coil configuration are shown in Fig. 2. Although the helicon source operating parameters were quite different for the different chambers, ion temperature anisotropy is clearly evident in both sets of measurements.

Ion temperature measurements in HELIXb in the eight-coil configuration were remarkably different.²³ Figure 3 shows both perpendicular and parallel ion temperatures measured on axis at position “B” (35 cm position) in HELIXb at two different driving frequencies with all other parameters the same. At 9 MHz, the ion temperatures increased with increasing magnetic field strength and there was no significant ion temperature anisotropy. At 13.5 MHz, a small temperature anisotropy existed at low magnetic field strengths but disappeared as the magnetic field strength was increased. The perpendicular ion temperatures peaked at a specific value of magnetic field strength and then decreased as the magnetic field strength increased further. The dependence of

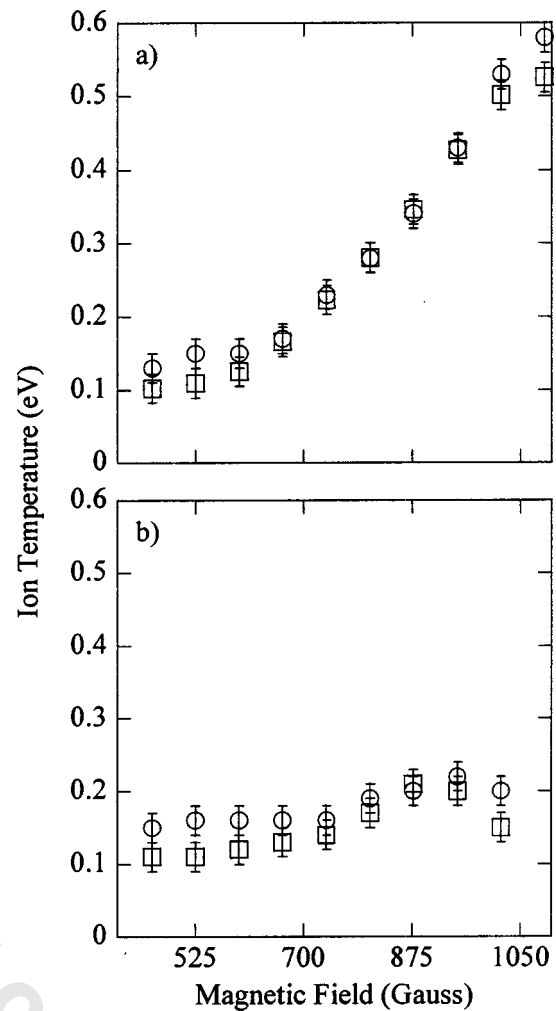


FIG. 3. (a) On axis (\circ) perpendicular and (\square) parallel ion temperature as a function of magnetic field strength for HELIXb in the eight-coil configuration at position “B” with a fill pressure of 6.7 mTorr, and 750 W of rf power for (a) a rf of 9 MHz and (b) a rf of 13.5 MHz.

the ion temperature on the magnetic field strength was clearly different for the two different rf driving frequencies even though the rf was hundreds of times greater than the ion cyclotron frequency.

The perpendicular and parallel ion temperature radial profiles at a rf of 9 MHz and a magnetic field strength of 1185 G are shown in Fig. 4. Although the ion temperature was isotropic at the center of the plasma, a substantial temperature anisotropy appeared at the plasma edge; the perpendicular ion temperature increased and the parallel ion temperature decreased. A flat or peaked at the edge perpendicular ion temperature profile could only result from either edge ion heating or a large axial thermal conductivity. As will be shown later, there is strong axial gradient in the perpendicular ion temperature profile. Therefore, these measurements demonstrated that the ions were heated at the edge of helicon sources and preferentially in the perpendicular direction.

The combined stainless steel and glass HELIXb vacuum chamber was specifically designed to permit ion temperature measurements at four different axial locations: -24 cm, 5 cm (position A), 35 cm (position B), and 60 cm (position C)

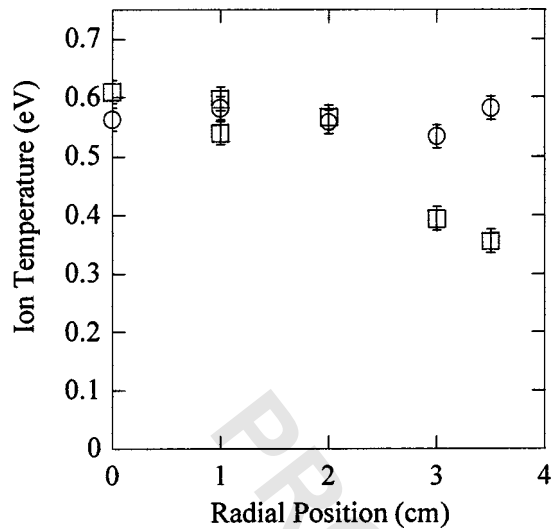


FIG. 4. (○) Perpendicular and (□) parallel ion temperatures vs radius for a fill pressure of 6.7 mTorr and a rf power of 750 W for a rf frequency of 9 MHz.

from the front edge of the antenna. Perpendicular ion temperatures in HELIXb in the ten-coil configuration at these four axial locations are shown in Fig. 5 for two different magnetic field strengths. At magnetic field strengths less than approximately 500 G, the ion temperature decreases monotonically with increasing distance from the antenna ($z > 0$). At magnetic field strengths greater than 500 G, the perpendicular ion temperatures peak downstream from the antenna ($z \sim 35$ cm). The perpendicular ion temperatures also peak downstream from the antenna in HELIXb in the eight-coil configuration.²³ As will be discussed shortly, the downstream ion temperature peak at higher magnetic field strengths is consistent with ion heating due to ion damping of the slow wave. Note that the ion temperatures on the back side of the antenna are lower than those in the front of the antenna in both cases, confirming a preferential direction for the energy

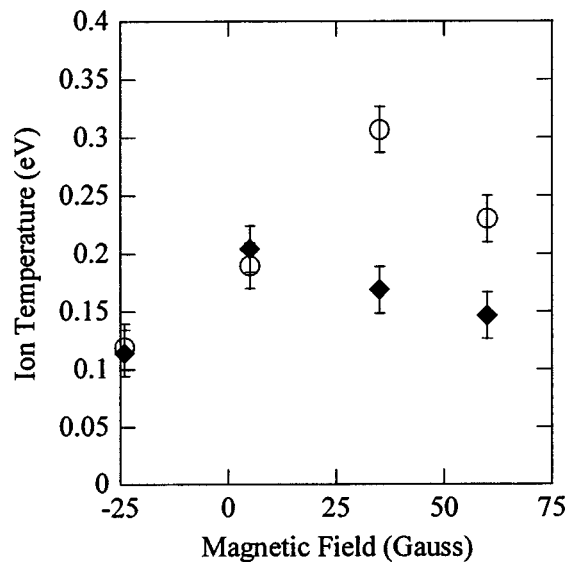


FIG. 5. Perpendicular ion temperatures in HELIXa at different axial locations for a magnetic field strength of (◆) 453 G and (○) 808 G.

deposition into the ions. Also note that near the antenna, the perpendicular ion temperatures still exceed what would be expected for simple collisional equilibration with the much hotter electrons.¹³ Since recent theoretical studies suggest that parametrically driven ion sound instabilities can explain observations of electron density maxima downstream of helicon antenna (previously attributed to simple pressure balance²⁴), we also considered the possibility that the parametrically driven ion sound turbulence could heat ions.^{25,26}

B. Slow wave ion heating

The mechanism responsible for perpendicular ion heating at the plasma edge was identified by careful investigation of the magnetic field strength and rf dependence of the ion heating. The first detailed measurements of the ion temperatures over a large range of rf driving frequencies and magnetic field strengths by Balkey *et al.*¹³ showed that the perpendicular ion temperatures were correlated with the lower hybrid frequency, but peaked at values roughly 70% below the lower hybrid frequency [Fig. 6(a)]. After the Balkey *et al.*¹³ experiments were performed in HELIXa, similar experiments were performed with HELIXb in the eight-coil configuration at location “B” [Fig. 6(b)].^{17,23} The perpendicular ion temperatures were again correlated with and peaked below the on axis lower hybrid frequency. However, the wider magnetic field and rf ranges attained in the HELIXb experiments showed a localized peak in perpendicular ion temperature at a specific set of magnetic field strength and rf values.

The cold plasma dispersion relationship has two solutions for wave frequencies near the lower hybrid frequency: the fast, “helicon,” wave and the slow, “Trivelpiece–Gould,” wave. Near the lower hybrid frequency, the perpendicular wave number for the slow wave undergoes a resonance while the perpendicular wave number for the helicon wave continues smoothly through the lower hybrid frequency.²⁷ The resonance in the perpendicular wave number of the slow wave can reduce the phase speed in the perpendicular direction to speeds that are close enough to the ion thermal speed such that ion Landau damping can occur.¹⁷ The result is an ion heating mechanism with a preferential direction with respect to the applied magnetic field.

The theoretically predicted characteristics of the slow wave are consistent with the measured spatial as well as rf and magnetic field strength dependencies of the perpendicular ion temperatures. First, the radial profile of both the perpendicular and parallel ion temperatures shown in Fig. 4 indicates that the largest anisotropic ion heating occurs near the edge of the plasma. Theory predicts that slow waves are primarily surface waves in helicon sources because they are strongly damped as the plasma density increases toward the center of a helicon source discharge.¹² Therefore, ion heating due to ion damping of slow waves would be expected to be largest at the edge of the plasma. Second, the decrease in lower hybrid frequency toward the edge of the plasma (due to density profile effects) results in a peak in the perpendicular wave number of the slow wave for a specific range of magnetic field strength and rf.^{17,23} Figure 7(a) shows the ion

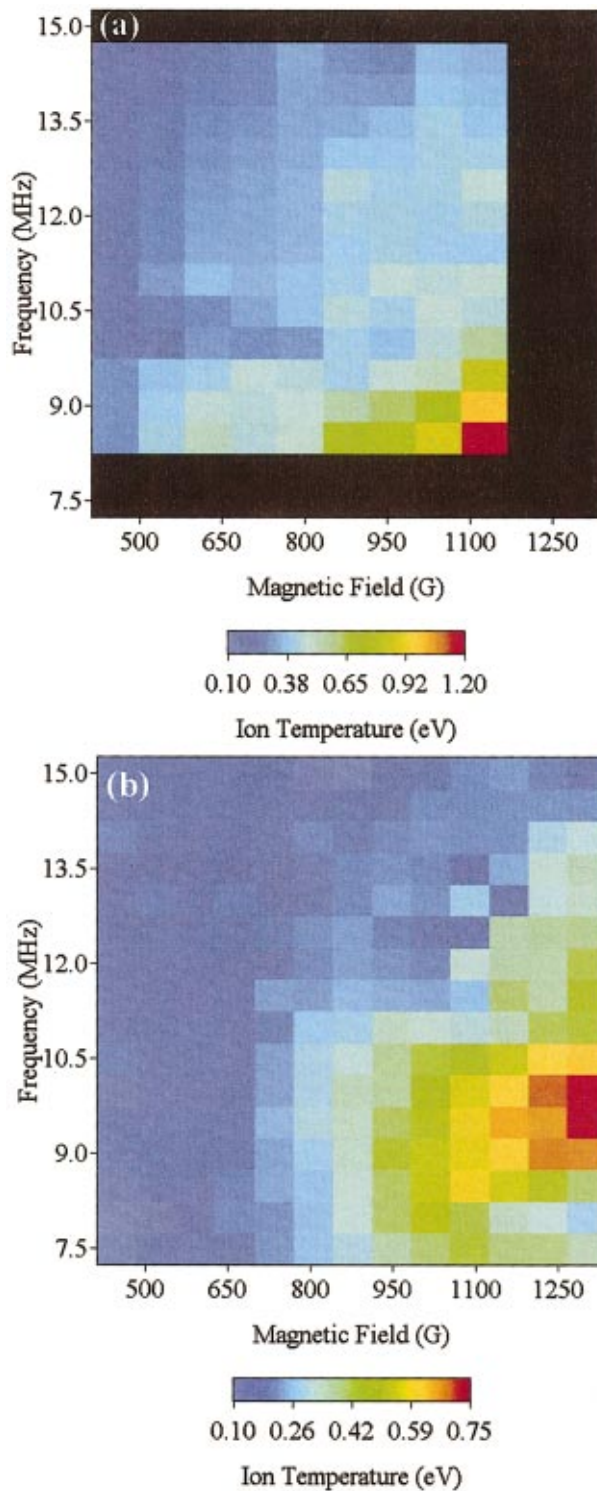


FIG. 6. (Color) (a) Ion temperatures as a function of rf and magnetic field strength in HELIXa. The region in black represents parameters at which the ion temperatures were not measured in HELIXa. (b) Ion temperatures as a function of rf and magnetic field strength in HELIXb in the eight-coil configuration at location “B.”

temperatures measured in HELIXb at the $z=35$ cm location in the eight-coil configuration. The solid white line indicates where the rf driving frequency equals the on-axis lower hybrid frequency for a fixed density of $2 \times 10^{12} \text{ cm}^{-3}$ (a typical on-axis density value) while the dashed line lies along the lower hybrid frequency curve for a fixed density of 1

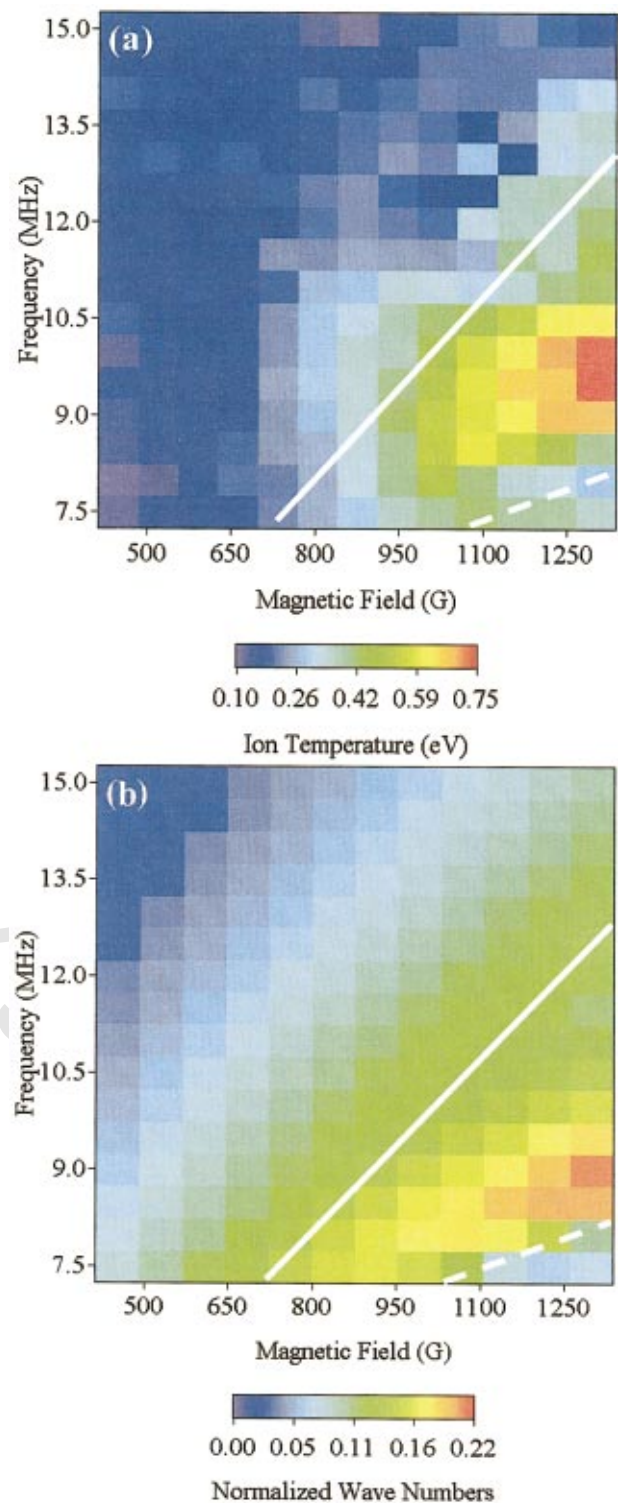


FIG. 7. (Color) (a) Ion temperatures measured at position “B” with HELIXb in the eight-coil configuration for a fill pressure of 6.7 mTorr and a rf power of 750 W. The white lines indicate where the rf driving frequency equals the lower hybrid frequency on axis (solid line) and at the plasma edge (dashed line) assuming plasma densities of 2×10^{12} and $1 \times 10^{11} \text{ cm}^{-3}$, respectively. (b) Calculated normalized wave numbers, $k_{\perp} v_{thi} / \omega$, from the cold plasma dispersion relation for the slow wave.

$\times 10^{11} \text{ cm}^{-3}$ (a typical edge density value). Although the plasma density varies with magnetic field strength, these values include the range of peak and edge densities for magnetic field strengths above 700 G. Using the cold plasma disper-

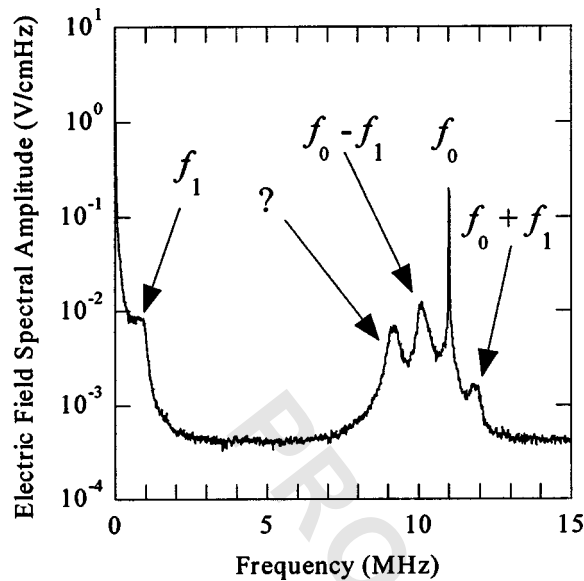


FIG. 8. Electrostatic fluctuation spectrum for a rf of 11 MHz and a magnetic field strength of 845 G at location “B” in HELIXb in the eight-coil configuration.

sion relationship of Cho including ion terms and collisions,²⁷ the magnitude of the slow wave perpendicular wave numbers in HELIXb as a function of magnetic field strength, rf, and plasma radius can be calculated using a series of simple homogeneous annuli with different plasma densities.¹⁷ For each rf and magnetic field strength, the perpendicular wave numbers were calculated at different radial positions using a parabolic density profile. The largest value of the perpendicular wave number across the plasma radius was recorded and plotted as a function of rf and magnetic field strength in Fig. 7(b). The peak values for the normalized wave numbers occur at the same values of rf and magnetic field strength as the peak perpendicular ion temperatures. Thus, the peak in perpendicular ion heating at the plasma edge and the rf and magnetic field strength dependencies of the ion heating are consistent with the conclusion that ion damping of slow waves in the edge of helicon sources is responsible for ion heating in helicon sources. In fact, except for the recent high frequency axial current measurements of Blackwell and Chen,²⁸ these ion heating measurements are the strongest experimental evidence to date for the existence of slow waves in helicon sources.²³ Direct measurements of such short wavelength waves, $\lambda < 1$ mm, are still beyond the capabilities of conventional helicon source diagnostics. We note, however, that recent microwave scattering experiments are close to being able to directly measure such short wavelength fluctuations in helicon sources.^{23,29}

C. Ion heating via parametric decay of the helicon wave

Electrostatic, parametrically driven instabilities have been observed in the HELIXb experiments.³⁰ Figure 8 shows the electric field power spectrum at position “B” in HELIXb in the eight-coil configuration. The 11 MHz pump wave, the forward and backward propagating waves (Stokes and anti-Stokes), and a low frequency beat wave are evident in the

power spectrum. A fifth spectral peak around 9 MHz is an experimental artifact and exists in all of our electrostatic power spectrum measurements. The power spectrum shows that the frequency matching condition, $f_2 = f_1 \pm f_0$, i.e., energy conservation is satisfied. Measurements of the wave numbers and magnetic field fluctuation power spectra confirm that the wave number matching condition, i.e., momentum conservation, is also satisfied and that the parametrically excited waves are purely electrostatic.³⁰ Radial measurements of the wave amplitudes show that the electrostatic waves are localized to the center of the plasma ($r < 3$ cm). The experimental data, including wave phase velocity and propagation direction measurements, are consistent with the interpretation that the parametrically excited waves (the sidebands) are electrostatic lower hybrid waves and the low frequency mode is an ion acoustic wave. The measured phase speeds of the electrostatic lower hybrid waves are too large for significant interaction with ions. However, the phase speed of the low frequency wave is on the order of three times the ion thermal velocity and ion damping of such waves is theoretically possible.

A comparison of the spectral amplitude of the low frequency wave as measured with the electrostatic probe at position “B” with the perpendicular ion temperatures at position “A” (near the antenna) is shown in Fig. 9 as a function of magnetic field strength and rf driving frequency. There is a rough correlation between the measured perpendicular ion temperatures and the amplitude of the low frequency waves. The wave numbers of the low frequency waves are larger at lower rf driving frequencies where the fluctuation amplitudes increase.³⁰ The larger wave numbers result in wave phase speeds within a factor of 2.5 of the ion thermal velocity. These measurements demonstrate that electrostatic waves are parametrically excited in HELIXb and that amplitude of the low frequency beat wave is largest (and the phase speeds smallest) for the same parameters at which the perpendicular ion temperatures near the rf antenna are largest.

IV. ION FLOW MEASUREMENTS

Ion heating is not the only dynamic ion process that can affect the operational parameters of helicon sources. Ion flows can enhance particle transport, drive instabilities, or perhaps even suppress transport by decorrelating instabilities. In HELIX, both axial and azimuthal (rotational) flows have been investigated. Classically, plasmas flow along magnetic fields at the sound speed. The more mobile electrons try to move ahead of the ions, but are held back by development of an ambipolar electric field. However, LIF measurements of ion flow in argon helicon plasmas indicate that the ions flow along the magnetic field at nearly the ion thermal velocity, which is roughly ten times smaller than the sound speed. Measurements of the azimuthal ion velocities have shown that the inner region of the plasma column rotates as a solid body and at the plasma edge the rotational velocity decreases. Such a sheared azimuthal velocity profile could excite Kelvin–Helmholtz or other shear driven instabilities in the edge region of helicon sources.

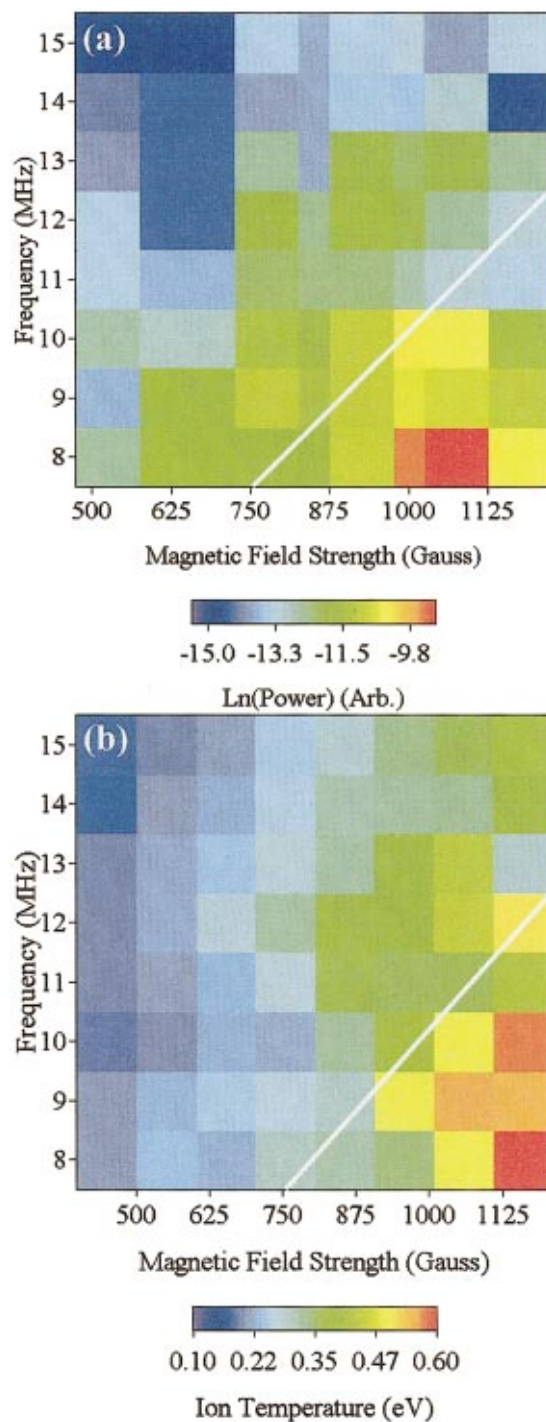


FIG. 9. (Color) (a) Signal amplitude of the low frequency wave at location "B" and (b) perpendicular ion temperatures at location "A" with HELIXb in the eight-coil configuration for a fill pressure of 6.7 mTorr and a rf power of 750 W.

A. Axial flows

In the past decade, a number of helicon sources have been constructed to investigate the possibility of using helicon sources as plasma sources for plasma thrusters,^{5,31} or directly as plasma thrusters.^{31,32} At WVU, an interest in instabilities driven by shear in the parallel flow³³⁻³⁷ motivated a series of experiments designed to investigate parallel flows in and exiting from helicon sources. The parallel velocities of

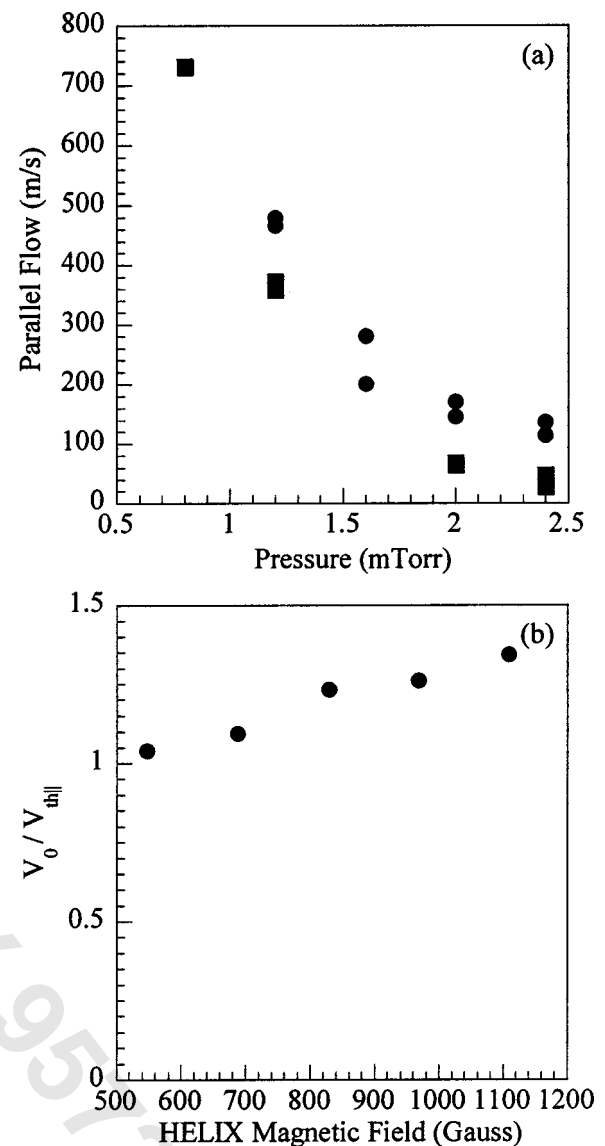


FIG. 10. (a) Parallel plasma flows vs fill pressure and (b) parallel plasma flows normalized to the ion thermal speed vs magnetic field strength for a fill pressure of 2 mTorr, a rf power of 750 W, and a rf of 9.5 MHz.

argon ions, and helium neutrals, in the WVU helicon source were determined by direct LIF measurements of the parallel ion velocity distribution functions.

Measurements of argon ion flow along the magnetic field inside the HELIXa chamber toward the LEIA chamber are shown in Fig. 10(a) as a function of neutral pressure. Parallel flow normalized to the parallel ion thermal speed as a function of magnetic field strength is shown in Fig. 10(b) for HELIXb in the ten-coil configuration. In both cases, the largest parallel flows inside the helicon source chamber are slightly larger than the parallel ion thermal speed, but considerably smaller than the ion sound speed ($C_s = (V_{te}/m_i)^{1/2}$). Less accurate measurements of parallel flow by Light *et al.* using a Mach probe yielded similar results.¹⁶ Thus, contrary to typical assumptions, ions flow out the end of linear helicon sources at roughly the ion thermal speed. The parallel ion flow profile is not uniform across the plasma diameter and flows maximized on axis and maximized at the plasma edge have both been observed in HELIXb.³⁸ The

shear in the parallel flow normalized to the ion gyrofrequency can be as large as $(dV/dx)(1/\Omega_i) \sim \pm 0.5$, large enough to drive both shear modified ion acoustic instabilities and shear modified ion cyclotron instabilities in thermally anisotropic plasmas.^{33–37}

What happens to the parallel ion flow as the magnetic field lines diverge into the expansion chamber is not well understood. Measurements in LEIA 1 m from the end of the helicon source find little to no evidence of parallel ion flow in argon plasmas. However, recent parallel flow experiments (using LIF on argon ions) found high-speed ion flows, on the order of 10 000 m/s, emanating from a small aperture at the end of the MNX helicon source.³¹ The aperture separates the high-power MNX helicon source from a larger expansion region with an expanding magnetic field geometry. If neutral braking due to charge-exchange collisions was responsible for the slowing of the parallel flow in the HELIX-LEIA experiments, a net flow in the neutral atoms might be expected. Yet measurements of neutral helium atoms (with LIF) also found no net flow in the region directly downstream from the HELIXa chamber during helium plasma operation. The dynamics of the ions (and neutrals) in the expansion region are the subject of a series of ongoing experiments at WVU using LIF probes that can scan along the plasma axis in LEIA and HELIX.

B. Rotational flows

In recent studies of the saturation of plasma density with increasing magnetic field in helicon sources, Light *et al.*¹⁶ proposed that enhanced diffusion to the excitation of resistive drift waves could explain the poor plasma confinement in helicon sources at high magnetic field strengths. Those studies ignored other potential instabilities, such as the Kelvin–Helmholtz instability, because there was no experimental evidence of plasma rotation in helicon sources. Measurements of the total perpendicular ion velocity in argon HELIXb plasmas are shown in Fig. 11 as a function of position in a cross-sectional plane for HELIXb in the ten-coil configuration. The flow vectors were measured by combining LIF measurements made along the vertical and horizontal directions at roughly 100 locations across a cross section of the plasma at location “C” (see Fig. 1). The flow vectors overlay a contour plot of metastable ion density, roughly proportional to the square of the plasma density. Based on previous measurements, the peak plasma density for these parameters (neutral pressure of 10.1 mTorr, rf power of 750 W, HELIX magnetic field strength of 716 G, and a rf of 9.5 MHz) is approximately $1 \times 10^{13} \text{ cm}^{-3}$. The ions clearly rotate around the central density peak and, except for a small region near $x = -2.0$ cm, the rotation frequency is nearly constant all the way to the plasma edge. The rotation direction is counterclockwise with respect to the magnetic field direction, i.e., in the opposite sense of the electron diamagnetic drift direction. To the best of our knowledge, these two-dimensional LIF measurements of the full azimuthal flow vector are the first such measurements in a plasma.

Azimuthal electron flow measurements have not been attempted. Given the difficulties associated with perpendicu-

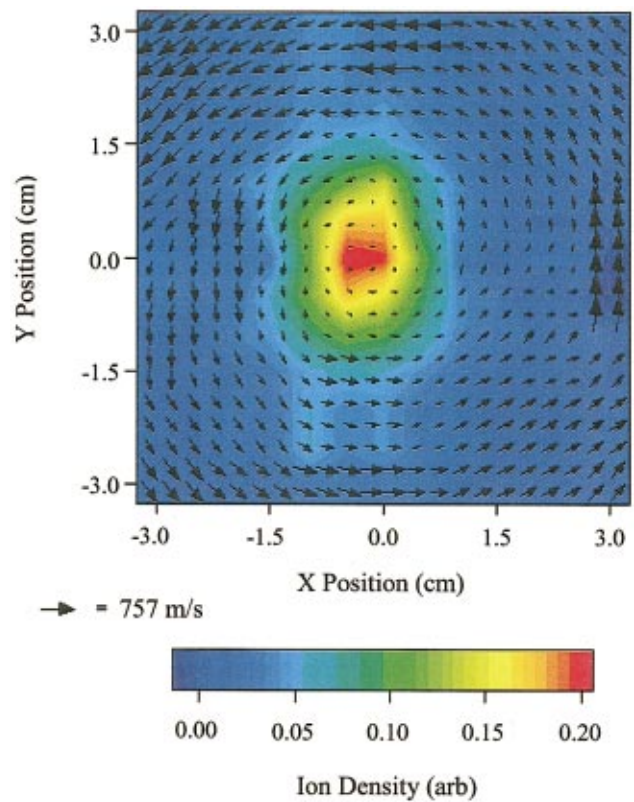


FIG. 11. (Color) Ion metastable density and rotational flow measurements versus position in a vertical plane cutting through the HELIX chamber at position “C” for a fill pressure of 10.1 mTorr, a rf power of 750 W, HELIX magnetic field strength of 716 G, and a rf of 9.5 MHz.

lar electron flow measurements and the harsh helicon source plasma environment (large thermal loads and large rf noise), we do not, at this time, have plans to measure the azimuthal electron flow. What is immediately clear from these preliminary ion flow measurements, however, is that significant rotational ion flows do exist in helicon sources.

V. DISCUSSION

The experimental measurements reported here have demonstrated that: ions in helicon sources are preferentially heated in the perpendicular direction; ion heating is maximum at some finite distance downstream from the antenna; and that the largest amount of ion heating downstream of the rf antenna occurs when the rf matches the local lower hybrid frequency at the edge of the plasma. Ion temperature radial profile measurements and comparison of ion temperature measurements as a function of rf and magnetic field strength with theoretical predictions for the perpendicular phase speed of the slow wave suggest that ion damping of slow waves is responsible for the observed ion heating downstream of the antenna. Close to the rf antenna, additional ion heating mechanisms appear to be important. Ion damping of parametrically driven waves is one possible mechanism that could provide for the observed ion heating near the antenna and there is some correlation between the observed ion heating and the amplitudes of the parametrically driven waves in the helicon source. As the downstream ion temperatures are typically at least 50% larger than the ion temperatures near

the antenna (see Fig. 5), the slow wave damping dominates the ion heating in the bulk of the helicon source.

When helicon sources are operated near the lower hybrid frequency, ion temperatures can reach 1.0 eV or larger and the ions then contain a significant fraction of the kinetic energy in the source, assuming $T_e \sim 4$ eV. Therefore, understanding how the rf energy ends up in the ions is critically important to understanding the power balance in helicon sources. As ion temperatures increase, the ion gyroradius increases and in plasmas with large ionization fractions dominated by ion-ion collisions, ion confinement times should correspondingly decrease. Since higher diffusion rates require more input power to maintain plasma densities, helicon source power balance calculations should also include the effects of collision driven radial transport.

If, as is true in most helicon sources, the ion-neutral collision frequency exceeds the ion-ion collision frequency, the mean free path of the ions in the neutral gas would govern the radial diffusion. In such cases, increased ion temperatures yield an increased ion-neutral collision frequency and radial transport of ions should decrease. Therefore, neutral density profile measurements are needed to fully understand the relationship between ion heating and radial diffusion in helicon sources. Neutral density profile measurements using LIF on argon and helium neutrals are currently under way at WVU.

Radial particle diffusion is the most likely process to establish radial electric fields and induce plasma rotation in helicon sources, although there are other processes that can create radial electric fields. The ion rotation measurements in HELIXb presented here clearly show solid body ion rotation for radii less than 3 cm. However, for some flow measurements not presented, shear in the azimuthal ion flow has been observed and could account for a variety of low frequency instabilities in helicon sources operating at high magnetic fields.¹⁶ Parallel flow measurements in HELIX indicate that ions flow out of the open end of helicon sources at roughly the parallel ion thermal speed and not at the ion sound speed. Since both centrally peaked and centrally depressed axial flow radial profiles have been observed, ion-neutral collisions do not appear to be solely responsible for the subsonic flow speeds observed in HELIX (the neutral density is expected to peak at the plasma edge and therefore one would expect the edge flow speed to always be lower than the on-axis flow if ion-neutral collisions slow the axial flow).

In summary, ion dynamics in helicon sources cannot be ignored when operating helicon sources at rf near the lower hybrid frequency. Typical assumptions that the ions are cold (approximately room temperature) or that the axial plasma flows are near the plasma sound speed have been shown to be untrue for the typical helicon operating parameters. Therefore, theoretical models of helicon sources should carefully consider the role of finite ion temperature and ion flow in helicon plasmas.

ACKNOWLEDGMENTS

We would like to thank the members of the WVU machine shop, Doug Mathess, Tom Milan, and Carl Weber, for

all of their efforts in constructing the HELIX/LEIA apparatus. We also acknowledge useful discussions with David Montgomery of Los Alamos National Laboratory and Vladimir Mikhailenko of Kharkov National University.

Work at WVU was performed with support from National Science Foundation Grant No. ATM-99988450 and the U.S. Department of Energy under Grant No. DE-FG02-97ER54420.

¹R.W. Boswell, Phys. Lett. **33A**, 457 (1970).

²R.W. Boswell, Phys. Lett. **55A**, 93 (1975).

³R.W. Boswell, Nature (London) **258**, 58 (1975).

⁴P.A. Keiter, E.E. Scime, M.M. Balkey, R. Boivin, J.L. Kline, and S.P. Gary, Phys. Plasmas **7**, 779 (2000).

⁵F.R. Chang Diaz, R.H. Goulding, R.D. Bengtson, F. Wally Baity, D. Sparks, R.G. Bussell, Jr., G.C. Barber, G. McCaskill, V.T. Jacobson, M.D. Carter, A.V. Ilin, and T.W. Glover, Fusion Technol. **35**, 243 (1999).

⁶J. Hanna and C. Watts, Phys. Plasmas **8**, 4251 (2001).

⁷C.M. Franck, O. Grulke, and T. Klingner, Phys. Plasmas **10**, 323 (2003).

⁸F.F. Chen, M.J. Hsieh, and M. Light, Plasma Sources Sci. Technol. **3**, 49 (1994).

⁹H.A. Blevin and P.J. Christiansen, Aust. J. Phys. **15**, 501 (1966).

¹⁰F.F. Chen and D. Arnush, Phys. Plasmas **4**, 3411 (1997).

¹¹G.G. Borg and R.W. Boswell, Phys. Plasmas **5**, 564 (1998).

¹²K.P. Shamrai and V.B. Taranov, Phys. Lett. A **204**, 139 (1995).

¹³M.M. Balkey, R.F. Boivin, J.L. Kline, and E.E. Scime, Plasma Sources Sci. Technol. **10**, 284 (2001).

¹⁴B. Davies, J. Plasma Phys. **4**, 43 (1970).

¹⁵F.F. Chen, Plasma Sources Sci. Technol. **7**, 458 (1998).

¹⁶M. Light, F.F. Chen, and P.L. Colestock, Phys. Plasmas **8**, 4675 (2001).

¹⁷J.L. Kline, E.E. Scime, R. Boivin, A. Keesee, and X. Sun, Plasma Sources Sci. Technol. **11**, 413 (2002).

¹⁸I.D. Sudit and F.F. Chen, Plasma Sources Sci. Technol. **3**, 162 (1994).

¹⁹E.E. Scime, M.M. Balkey, R. Boivin, and J.L. Kline, Rev. Sci. Instrum. **72**, 1672 (2000).

²⁰D.H. Hill, S. Fornaca, and M.G. Wickham, Rev. Sci. Instrum. **54**, 309 (1983).

²¹R.A. Stern and J.A. Johnson III, Phys. Rev. Lett. **34**, 1548 (1975).

²²E.E. Scime, P.A. Keiter, M.W. Zintl, M.M. Balkey, J.L. Kline, and M.E. Koepke, Plasma Sources Sci. Technol. **7**, 186 (1998).

²³J.L. Kline, E.E. Scime, R.F. Boivin, A. Keesee, and X. Sun, Phys. Rev. Lett. **88**, 195002 (2002).

²⁴I.D. Sudit and F.F. Chen, Plasma Sources Sci. Technol. **5**, 43 (1996).

²⁵A.I. Akhiezer, V.S. Mikhailenko, and K.N. Stepanov, Ukr. Fiz. Zh. **42**, 990 (1997).

²⁶A.I. Akhiezer, V.S. Mikhailenko, and K.N. Stepanov, Phys. Lett. A **245**, 117 (1998).

²⁷S. Cho, Phys. Plasmas **7**, 417 (2000).

²⁸D.D. Blackwell, T.G. Madziwa, D. Arnush, and F.F. Chen, Phys. Rev. Lett. **88**, 145002 (2002).

²⁹N.M. Kaganskaya, M. Krämer, and V.L. Selenin, Phys. Plasmas **8**, 4694 (2001).

³⁰J.L. Kline and E.E. Scime, Phys. Plasmas **10**, 135 (2003).

³¹S.A. Cohen, N.S. Siefert, S. Stange, E.E. Scime, R.F. Boivin, and F. Levinton, "Supersonic plasma stream generation by a helicon discharge in a magnetic-mirror configuration," to appear in Phys. Plasmas (2003).

³²E.B. Hooper, Phys. Plasmas **2**, 4563 (1995).

³³G. Ganguli, S. Slinker, V. Gavrishchaka, and W. Scales, Phys. Plasmas **9**, 2321 (2002).

³⁴V. Gavrishchaka, M.E. Koepke, and G. Ganguli, Phys. Plasmas **3**, 3091 (1996).

³⁵V.V. Gavrishchaka, S.B. Ganguli, and G.I. Ganguli, Phys. Rev. Lett. **80**, 728 (1998).

³⁶R.S. Spangler, E.E. Scime, and G.I. Ganguli, Phys. Plasmas **9**, 2526 (2002).

³⁷E.E. Scime, A.M. Keesee, R.S. Spangler, M.E. Koepke, C. Teodorescu, and E. W. Reynolds, Phys. Plasmas **9**, 4399 (2002).

³⁸X. Sun, A. Keesee, J. Kline, and E. E. Scime, Bull. Am. Phys. Soc. **47**, 32 (2002).